

AD-A162 392

FUNDAMENTAL EXPERIMENTS AT LIQUID HELIUM TEMPERATURES
(LOW TEMPERATURE ST. (U) STANFORD UNIV CA DEPT OF
PHYSICS W M FAIRBANK ET AL 30 SEP 84 AFOSR-TR-85-1068

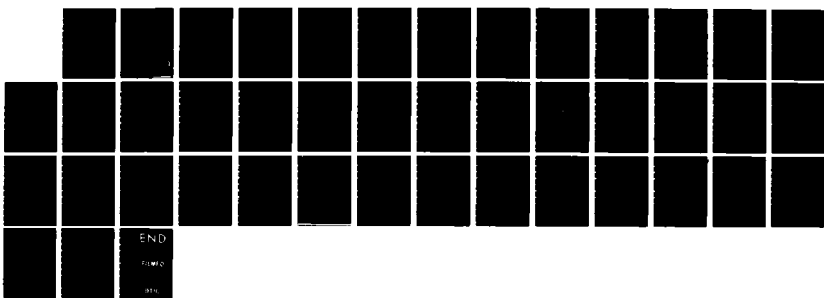
1/1

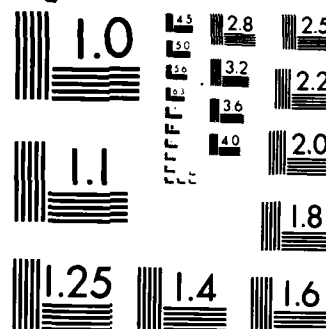
UNCLASSIFIED

AFOSR-80-0026

F/G 20/3

NL



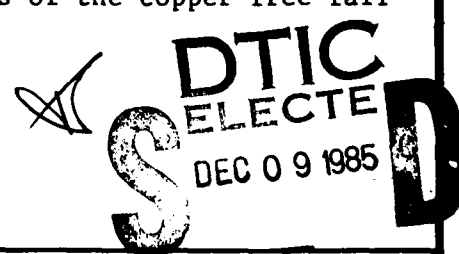


MICROCOPY RESOLUTION TEST CHART
NATIONAL BUREAU OF STANDARDS-1963-A

AD-A162 392

DOCUMENTATION PAGE

2

1a. REPC		1b. RESTRICTIVE MARKINGS				
Unclassified						
2a. SECURITY CLASSIFICATION AUTHORITY		3. DISTRIBUTION/AVAILABILITY OF REPORT				
		Approved for public release; Distribution unlimited				
2b. DECLASSIFICATION/DOWNGRADING SCHEDULE						
4. PERFORMING ORGANIZATION REPORT NUMBER(S)		5. MONITORING ORGANIZATION REPORT NUMBER(S) AFOSR-TR- 85-1068				
6a. NAME OF PERFORMING ORGANIZATION Stanford University		6b. OFFICE SYMBOL (If applicable)				
		7a. NAME OF MONITORING ORGANIZATION AFOSR/NP				
6c. ADDRESS (City, State and ZIP Code) Department of Physics Stanford University Stanford, California 94305		7b. ADDRESS (City, State and ZIP Code) Building 410 Bolling AFB, DC 20332-6448				
8a. NAME OF FUNDING/SPONSORING ORGANIZATION AFOSR		8b. OFFICE SYMBOL (If applicable) NP				
8c. ADDRESS (City, State and ZIP Code) Building 410 Bolling AFB, DC 20332-6448		9. PROCUREMENT INSTRUMENT IDENTIFICATION NUMBER AFOSR-80-0026				
10. SOURCE OF FUNDING NOS.						
		PROGRAM ELEMENT NO. 61102F	PROJECT NO. 2301	TASK NO. A9	WORK UNIT NO. N/A	
Fundamental Experiments at Liquid Helium Temperatures (Low Temperature Studies of Anomalous Surface Shielding and Related Phenomena)						
12. PERSONAL AUTHOR(S) William M. Fairbank, John M. J. Madey						
13a. TYPE OF REPORT FINAL	13b. TIME COVERED FROM 1/10/79 TO 30/9/84		14. DATE OF REPORT (Yr., Mo., Day) 30 Sep 84	15. PAGE COUNT 40		
16. SUPPLEMENTARY NOTATION						
17. COSATI CODES		18. SUBJECT TERMS (Continue on reverse if necessary and identify by block number)				
FIELD	GROUP	SUB. GR.				
19. ABSTRACT (Continue on reverse if necessary and identify by block number)						
During the research grant period, two graduate students received their Ph. D. and three papers were published in archival journals. It was found that an electron in an evacuated dewar, falling under the influence of gravity, experiences a net force of $10(-5)$ to $10(-7)$ V/m from 300 to about 4.5 degrees-K. At 4.5 degrees-K there is a transition to a net force of zero to within $6 \times 10(-12)$ V/m. This effect has been traced to the creation of a 2-D surface plasma of free electrons on the walls of the copper free-fall tube at the transition temperature.						
 DTIC SELECTED DEC 09 1985						
20. DISTRIBUTION/AVAILABILITY OF ABSTRACT UNCLASSIFIED/UNLIMITED <input checked="" type="checkbox"/> SAME AS RPT. <input checked="" type="checkbox"/> DTIC USERS <input type="checkbox"/>			21. ABSTRACT SECURITY CLASSIFICATION E			
22a. NAME OF RESPONSIBLE INDIVIDUAL ROBERT J. BARKER			22b. TELEPHONE NUMBER (Include Area Code) (202)-767-5011	22c. OFFICE SYMBOL NP		

Department of Physics
Stanford University
Stanford, California 94305

FINAL SCIENTIFIC REPORT

to the

AIR FORCE OFFICE OF SCIENTIFIC RESEARCH

for

FUNDAMENTAL EXPERIMENTS AT LIQUID HELIUM TEMPERATURES

(LOW TEMPERATURE STUDIES OF ANOMALOUS SURFACE SHIELDING AND RELATED
PHENOMENA)

Air Force Contract # AFOSR 80-0026

1 October 1979 - 30 September 1984

Principal Investigator:
William M. Fairbank
Professor of Physics

Co-Principal Investigator:
John M. J. Madey
Professor (Research)

Accession For	
NTIS	GRA&I <input checked="" type="checkbox"/>
DTIC TAB	<input type="checkbox"/>
Unannounced	<input type="checkbox"/>
Justification	
By _____	
Distribution/ _____	
Availability Codes	
Dist	Avail and/or Special
A-1	

Approved for public release;
distribution unlimited.

research, the researcher's investigation

During the time of this ~~report~~ period, we have been engaged in four experiments bearing on the nature of the anomalous surface effect found on the surface of copper in the experiment to measure the force of gravity on the electron. The following is a list of the graduate students involved in the project.

1) Christopher Waters - Received his Ph.D. - title of dissertation: "Microwave Surface Impedance Studies on Copper at Low Temperature".

2) Glen Westenskow - Received his Ph.D. - title of dissertation: "Confinement and Thermalization of Low Energy Electrons: The Development of a Low-Energy Ground-State Electron/Positron Source" (see Appendix 6).

3) John Henderson - currently completing his thesis on the electron free fall experiment.

4) Wayne Rigby - completing his thesis on experiments on copper and aluminum with microwave cavity.

5) Mark Rzchowski - halfway through his thesis on "Infrared Resolution of Low Temperature Surface Potential."

The following papers are included in the Appendix: Three papers which have been published under the grant; two more papers which are to be published by Freeman Press in an upcoming book entitled Near Zero: New Frontiers of Physics; and a review paper entitled "Near Zero, A Frontier of Physics," which includes a description of the positron/electron free fall experiment.

The research under this grant grew out of an experiment to determine the force of gravity on individual electrons and positrons.

In that experiment W. M. Fairbank and F. C. Witteborn found the net force exerted on an electron travelling along the axis of a vertical copper tube to be zero to within $\pm 6 \times 10^{-12}$ V/m. From 300 K to ~4.5 K the net force is found to be 10^{-5} to 10^{-7} V/m. At 4.5 K there is a transition to the value seen by Fairbank and Witteborn. We are now performing several tests on metallic surface shielding effects at low temperatures, to specify what conditions are necessary to obtain the dramatic shielding increase that was observed on a copper surface near 4.5 K.

The work under this grant has addressed this problem using two techniques in addition to the free fall experiment. One involves measuring to one part in 10^{10} the frequency of a microwave cavity as a function of temperature and the second involves measuring the patch effect field on a rotating sample as a function of temperature. The experiments with falling electrons are discussed in the publications included in Appendices 1 and 2. The experiments with the copper cavity are discussed in the publications included in Appendices 3 and 4, and the experiments to look directly at the patch effect field on a rotating sample are discussed in Appendix 5. The experiments to obtain a low energy source of positrons for the free fall experiment is discussed in Glen Westenskow's Ph.D. thesis (Appendix 6). A brief summary of the latest status of these experiments is included below.

SPATIAL RESOLUTION OF LOW TEMPERATURE SURFACE POTENTIAL

I. INTRODUCTION

This experiment is designed to investigate directly an electron gas (conducting layer) which may exist on or outside the surface of many oxide-covered metals⁽¹⁻⁴⁾. This could be formed by oxide surface states undergoing a transition to a conducting gas⁽¹⁾ or electrons bound in their image potential outside a conducting surface^(2,5,6). Unpopulated image potential states have recently been observed on clean metals with inverse photoemission techniques.^(7,8)

Such a conducting layer would tend to shield any variations of electric field below it,^(1,2) and hence to smooth the surface potential measured beyond the layer. The drift tube experiment⁽⁴⁾ gives evidence of surface shielding on copper drift tubes but with little flexibility to examine different surfaces. The microwave cavity work described in the following section also shows an effect at low temperature. In order to independently verify this surface shielding effect in a straightforward and accessible manner, we have developed an ultra-high vacuum cryogenic apparatus to spatially resolve the temperature-dependent surface potentials of metals. This modified Kelvin probe described below is extremely surface sensitive and does not disturb the electronic structure as do other methods.^(9,10)

The technique used here (described more fully in Appendix 5) is a modification of the Kelvin method for measuring contact potential differences between two materials. In the Kelvin method one uses a parallel plate capacitor whose separation varies in time. The time-dependent (contact) potential difference between the plates and the

varying capacitance force a time-dependent charge to appear on the capacitor. This charge flow appears as an external current which can then be amplified.

In the place of a varying capacitance we substitute a periodic variation in the contact potential difference while keeping the capacitance fixed, resulting also in a measureable charge flow. We obtain the necessary potential variation by replacing the reference plate of the capacitor with a much smaller reference electrode, so that only a small portion of the sample surface is sensed at any one time. The sample is then rotated above this electrode so that the region probed varies continuously in time, describing an annulus on the sample surface. In the case of an electrically inhomogeneous surface, such as polycrystalline copper with different work functions on distinct crystal faces, the surface potential is a function of position, creating a time-varying contact potential difference as it rotates above the stationary reference electrode. (A schematic diagram of the apparatus appears as Figure 1 of Appendix 5). Instead of moving a vibrating electrode along the sample surface to get spatial resolution using the Kelvin method, we use rotary motion of the sample to substitute for a capacitance variation as well as to obtain spatial resolution.

II. SENSITIVITY

The sensitivity of the apparatus is dramatically increased by signal averaging. We currently rotate the sample between three and four Hertz, so that a standard run of 1000 revolutions takes approximately four minutes. Hence we obtain a signal to noise ratio thirty times better than that for a single rotation. Faster rotation rates, hence greater signal to noise ratios in a shorter time, require a rotary feedthrough capable of turning faster than the 300 rpm limit of the present model.

Although the signal is processed through a relatively complicated amplifier chain whose stray impedances at the level of the cooled preamplifier (see Section III) are important, the overall gain beyond the corner frequency is approximately 2.4 at an electrode spacing of 0.1 mm and an electrode diameter of 1 mm. An rms noise level has been obtained by subtracting two identical runs of 1000 rotations each. The difference indicates that the rms noise level is 0.2 digitization units of the A/D converter, or roughly 1 mV. This then corresponds to 400 μ V at the surface.

Such a sensitivity is much better than previous attempts of localized measurements⁽¹¹⁻¹⁴⁾, which have all operated at room temperature. In order to gain spatial sensitivity, the electrode diameter can be reduced to 100 μ (equivalent to 38 gauge wire). This reduces the signal by a factor of one hundred, bringing the effective noise level to 80 mV. This can be reduced by averaging over more rotations, although this level of sensitivity is adequate to

differentiate, for instance, between crystal faces - a difference of about 100 mV. ⁽¹⁵⁾

III. PRELIMINARY LOW TEMPERATURE WORK

Because a high impedance preamplifier must be physically close to the sample to prevent signal loss and noise pickup, it must in this case also operate at a low temperature. An amplifier working at approximately 100 K has been developed and integrated into the experiment described above. Based on a Siliconix 2N4867A JFET which has its highest gain at this temperature, the amplifier is isolated from the bath in its own vacuum space and is warmed by a resistance heater.

As a test sample, one strip of gold and one of platinum, each 1000 Angstroms thick, were sputtered 180 degrees apart from another on a stainless steel substrate. Data from one thousand rotations of the sample at atmospheric pressure (and ambient temperature) is shown in Figure 1 (this figure does not show a full 360 degree rotation). The peaks due to the gold and platinum strips are clearly shown.

Prior to a low temperature run, the system is first evacuated by a pair of adsorption pumps, then brought to a pressure of approximately 10^{-9} torr with an ion pump which is left continuously running. The system is then free from hydrocarbon contamination, and the pressure drops considerably when it is cooled.

Data from a preliminary run at low temperatures are shown in Figures 2 and 3. The distorted peaks and additional structure are presumably due to dust particles on the sample. Data at room temperature reproduces that at nitrogen temperature to within the noise, as does data taken again at nitrogen after warming from helium.

Since a calibration method for the amplifier was not yet developed, the relative magnitudes of the nitrogen and helium temperature data are unknown. If, however, we scale them so that the large peaks have the same magnitude (as in Figures 2 and 3), we can subtract them to get the temperature dependent surface potential change shown in Figure 4. The major difference peaks at the location of the platinum strip. One could then conclude that the temperature dependence is due to differences between the strip and the substrate.

In summary, the preliminary runs have demonstrated that the apparatus works at low temperatures and in ultra-high vacuum. The sensitivity is approximately 400 μ V with an electrode diameter of one millimeter. However, data has been taken only at three temperatures: ambient, liquid nitrogen, and liquid helium pumped to approximately 1.8 K without any attempt to regulate the temperature.

IV. PROPOSED RESEARCH

In the immediate future we plan to run at low temperatures with accurate thermometry and a method of introducing a calibration signal in place of the surface potential. This calibration will clear up the difficulties of scaling discussed in the last section. An added resistance heater and temperature controller allow us to take continuous temperature measurements rather than points at the bath temperature.

With this apparatus we can easily interchange and characterize different surfaces, and can proceed with a direct examination of copper and aluminum surfaces in hopes of elucidating the microwave cavity⁽³⁾ and drift tube⁽⁴⁾ experiments. Spatial resolution seems essential, and although the average surface potential of some metals have been measured

at low temperature^(16,17) the local variations with temperature have not been investigated. Bardeen's⁽¹⁾ explanation of the drift tube results suggests local variations to be important.

FIGURE CAPTIONS

Figure 1: Surface potential averaged over 1000 revolutions of the test sample at ambient temperature and pressure. The peaks due to the gold and platinum strips (1000 Å thick) over the stainless steel substrate are clearly shown.

Figure 2: Surface potential averaged over 1000 revolutions of the test sample of liquid helium temperature and pressure $< 10^{-9}$ torr. The additional structure over fig. 1 may be due to dust particles on the surface.

Figure 3: Surface potential averaged over 1000 revolutions of the test sample at liquid nitrogen temperature and pressure $< 10^{-9}$ torr. Note the change in surface potential at the location of the first peak of Figure 1. This was reproducible to within the noise after warming from liquid helium.

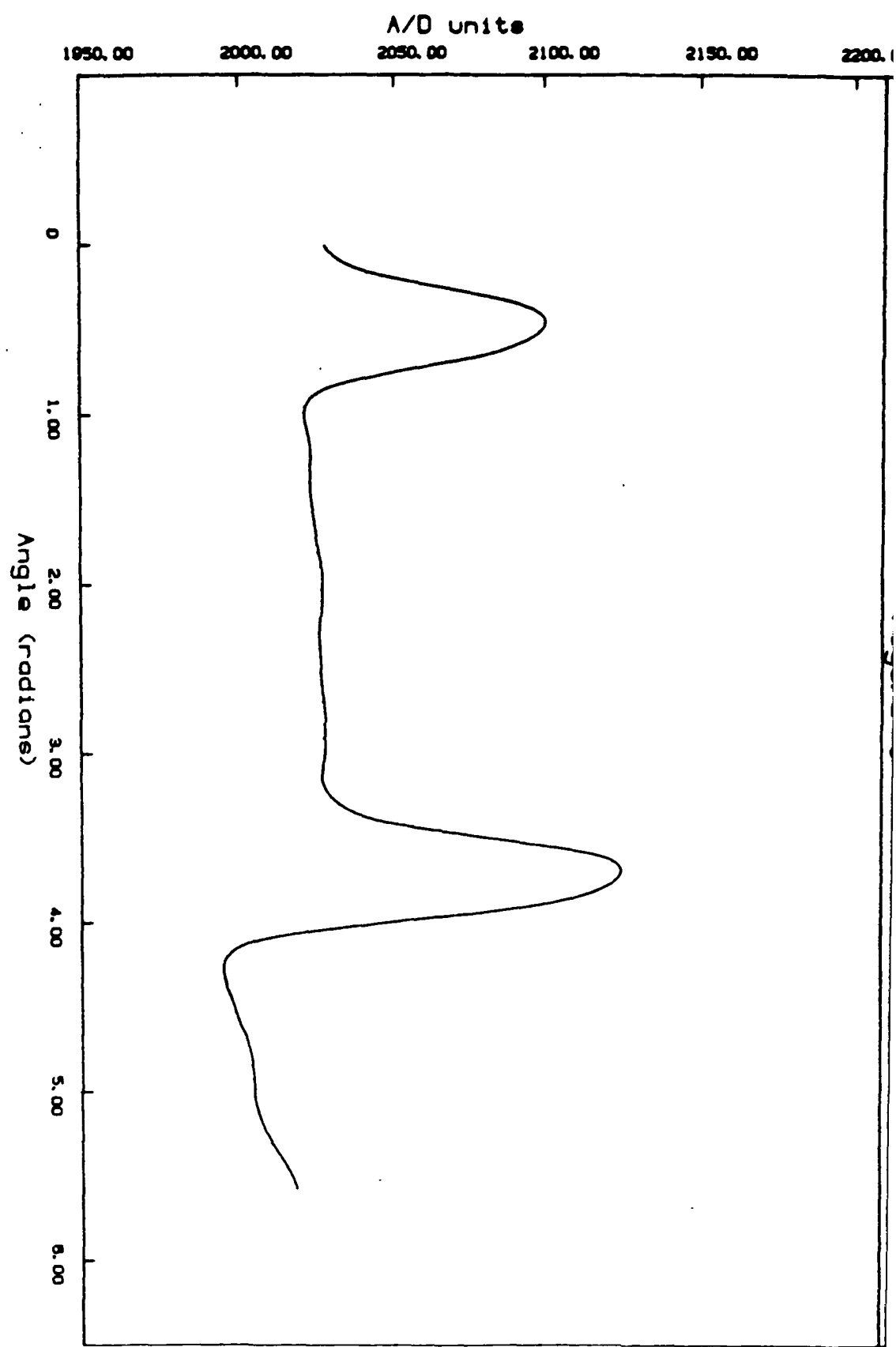


Figure 1: Surface potential averaged over 1000 revolutions of the test sample at ambient temperature and pressure. The peaks due to the gold and platinum strips (1000 Å thick) over the stainless steel substrate are clearly shown.

Figure 2

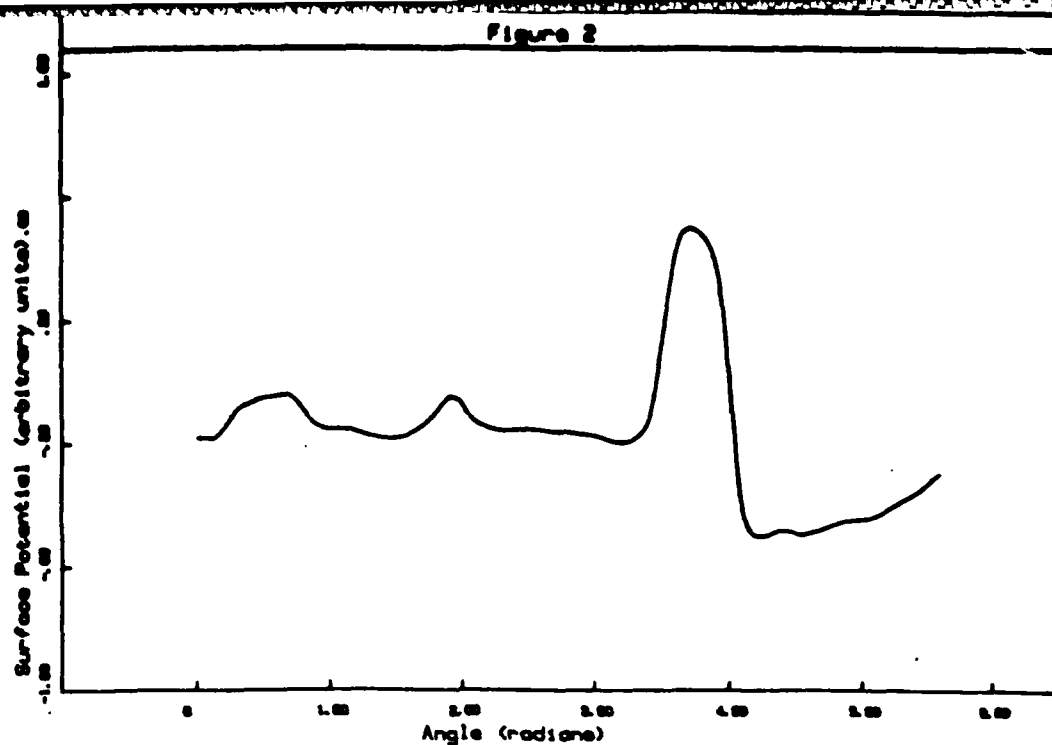


Figure 2: Surface potential averaged over 1000 revolutions of the test sample of liquid helium temperature and pressure $< 10^{-9}$ torr. The additional structure over fig. 1 may be due to dust particles on the surface.

Figure 3

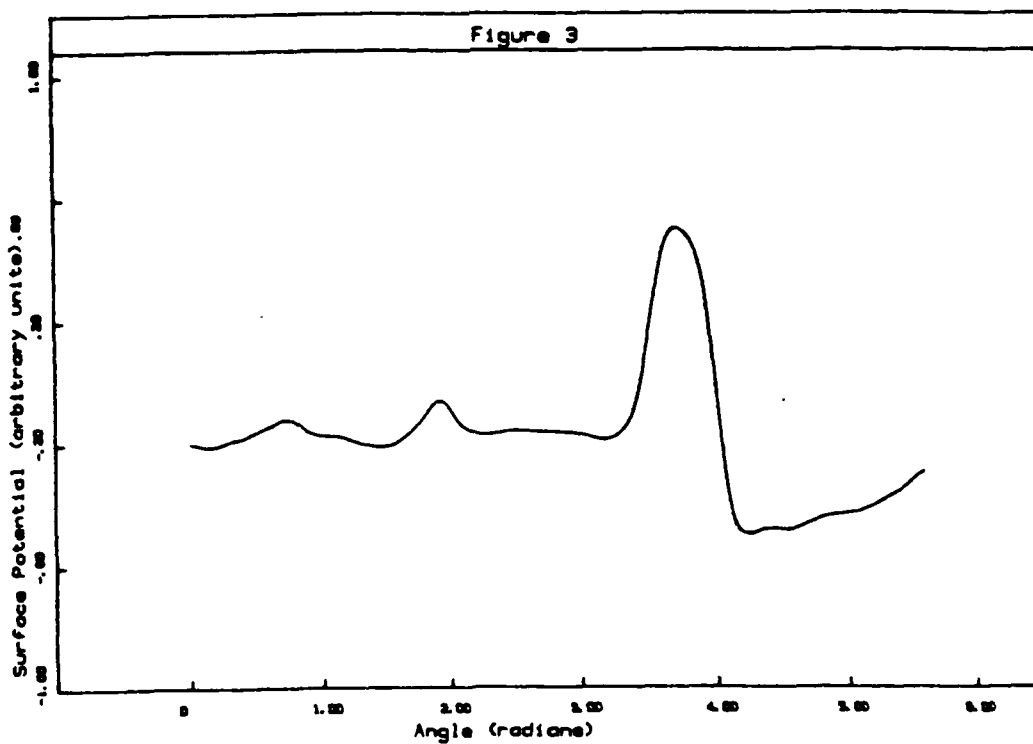


Figure 3: Surface potential averaged over 1000 revolutions of the test sample at liquid nitrogen temperature and pressure $< 10^{-9}$ torr. Note the change in surface potential at the location of the first peak of Figure 1. This was reproducible to within the noise after warming from liquid helium.

THE MICROWAVE CAVITY EXPERIMENT

In this section we will discuss the microwave cavity experiment, describing the low temperature anomalies and the magnetic resonance that we have observed, the implications these measurements have for a model, and what further experiments we plan to make.

APPARATUS

A cylindrical microwave cavity, operated at 9.12 GHz in the TE011 mode, is enclosed in a vacuum can which sits in liquid helium. The cavity temperature can be varied over the range 2-40 K and is measured with a calibrated germanium thermometer. A pair of superconducting Helmholtz magnets outside the vacuum space allow fields of 0-4 kG to be applied independently along the cavity axis and in a direction perpendicular to this axis. A feedback system locks a tunable microwave oscillator to the cavity resonance. The resonant frequency can be tracked with a precision of better than one hertz (i.e., one part in 10^{10}).

FREQUENCY VERSUS TEMPERATURE MEASUREMENTS

One of the principal measurements made with the apparatus is the resonant frequency as a function of temperature, $f(T)$. The dominant temperature dependence is due to thermal expansion. This background can be subtracted from the data by fitting the known form of thermal expansion at low temperatures for metals, which gives $f(T) = f_0 + aT^2 + bT^4$. Changes in the surface impedance

$$Z = (4\pi/c)(E_{\text{tang}}/H_{\text{tang}})_{\text{surface}}$$

produce frequency shifts $\Delta f \propto \Delta \chi$, where $\chi = \text{Im}(Z)$. (The real part of Z determines the cavity Q .) Thus anything which affects the electromagnetic fields at the cavity surface perturbs the cavity frequency. In particular, a metal-insulator transition involving $10^{13}/\text{cm}^2$ electrons on the surface gives a frequency shift of 16 Hz, which is easily observable.

We have observed anomalies in over half the samples tested, both copper and aluminum. The magnitude of the anomalies ranges from about 1 Hz to 100 Hz. Figure 5 shows the anomalous part of the frequency shift for an aluminum sample. Figure 6 shows two anomalies in a copper sample, one near 3.8 K as in the aluminum sample and a second near 7.2 K. These anomalies are reproducible and stable; one sample showed no change in runs over a year apart.

The anomaly below 3.8 K is suppressed by an external magnetic field, shifting down in temperature with increasing field until, at about 200 G, the frequency curve follows the thermal expansion form down to 2 K. Fields both parallel and perpendicular to the sample suppress the effect. The 7 K anomaly seems to have a much higher field dependence; we have not yet measured it accurately.

To confirm that these anomalies are indeed a surface effect, we deliberately contaminated the surface of one copper sample with vacuum grease. Figure 7 shows that the 7 K anomaly was completely suppressed and that the 3.8 K anomaly was reduced by a factor of four. (Note that the temperature derivative is plotted.)

DISCUSSION

The original model proposed for this experiment was that of a two-dimensional layer of electrons bound to the metal surface by the electrostatic image potential but trapped outside it by an oxide layer barrier, in analogy with the case of electrons trapped on the surface of liquid helium⁽⁶⁾. Bardeen⁽¹⁾ has suggested that electrons localized on adsorbed oxygen atoms on the surface might undergo a metal-insulator transition at low temperatures, forming a surface layer of nearly free electrons.

Such quasi two-dimensional electron layers are known to exist in a variety of systems and are currently of great interest.⁽¹⁸⁾ Besides electrons on bulk helium, they include electrons on thin films of helium above metals⁽¹⁹⁾, natural accumulation layers on ZnO⁽²⁰⁾ and at germanium bicrystal interfaces⁽²¹⁾, and surface bands on clean metals⁽²²⁾. For the case of clean metals, in particular, there has been a recent claim to have observed image-potential-induced surface states⁽²³⁾. This work was done on atomically clean copper samples; the states lie above the Fermi energy (that is, normally unoccupied).

None of these systems is known to undergo a metal-insulator transition as a function of temperature. In the electron-helium systems, however, a phase transition from a free electron gas to a low temperature lattice phase has been observed⁽²⁴⁾. In our experiments, one possibility is that we are observing phase transitions in a free electron gas that is always present on these surfaces. Recently we began a series of experiments to look for such a free electron state directly, using cyclotron resonance.

RESONANCE AT HIGH MAGNETIC FIELDS

We have found resonances in all three samples we have so far tested - in aluminum, copper, and a gold-plated cavity. Figure 8 is typical, showing the large frequency shift and increased power absorption occurring at resonance. The frequency shifts are as much as 100 KHz (in contrast to the 100 Hz shifts in zero magnetic field) and the power adsorbed in the cavity increases by as much as 30%. The resonance occurs within 5% of the cyclotron field for free electrons (3200 G) for fields perpendicular to the cavity endplates. (This is within the uncertainty of the magnet calibration.) The line width is of the order of 1%, implying a long scattering time of about 10^{-9} seconds.

One of the most intriguing features of the resonance is that it only appears above a certain minimum incident microwave power level. Figure 9 shows the decrease in the magnitude of the resonance as a function of incident power. The peak heights for the two features seen in Figure 8 are plotted separately. The threshold corresponds to a power absorption in the cavity of about one milliwatt.

We believe that this can be explained within the image-potential model⁽²⁵⁾. An image potential $1/x$ generates a set of free electron bands with a hydrogen-like spectrum perpendicular to the surface - free electron-like in the direction parallel to the surface, but localized in discrete states perpendicular to the surface. If the lowest-lying states (those populated in thermal equilibrium) have short scattering times because of their increased interaction with the surface, then no cyclotron resonance will be observed for these states. (The condition

$\omega\tau > 1$, where ω is the frequency and τ is the scattering time, is not satisfied.) But absorption (proportional to the incident power) near the resonant field will tend to populate the higher energy states. If these have sufficiently long scattering times and are sufficiently populated, then a resonance will be observed.

Two additional features of the data support such an interpretation. The "tails" of the resonance are much smaller than can be explained by cyclotron resonance with a single scattering time. And near the power threshold, the system seems to "switch" erratically from the nonresonant to the resonant state (see Figure 10).

We admitted helium gas to the system in one run with the expectation that this should decrease the scattering time and thus perturb the resonance. This was indeed observed. The line was broadened, the power threshold increased, and the switching effects magnified - all consistent with the model.

We hope to be able to make this model quantitative. It should be possible to extract much useful information from the resonance, such as the density of surface electrons and their scattering times.

FUTURE EXPERIMENTS

There are a number of experiments that we would like to perform in the near future. We would like to know how the resonance depends on the orientation of the magnetic field with respect to the metal surface. For electrons on helium, the resonance was found to depend only on the perpendicular components of the field, and this was taken to be strong evidence for the two-dimensional nature of the surface states.⁽²⁶⁾

We would also like to set up a room temperature magnet. This would have at least three advantages. It would allow the resonance to be investigated over the full temperature range from 2-300 K (to date we have observed the resonance at temperatures up to 40 K). Much better field homogeneity would be possible, allowing the undistorted line shape to be measured. And the accuracy with which the resonant field is known could be improved, which gives a better number for the effective mass of the surface electrons.

Finally, it would be advantageous to work in a bakeable, ultra-high vacuum system. Inert gas sputtering with an ion gun can be used to prepare an atomically clean sample surface. Since we know that the presence of surface contaminants can strongly influence the effects we see, it would simplify the interpretation to work with as clean a surface as practical. In addition, in situ deposition of oxides would allow us to determine whether oxide thickness is a crucial parameter for the existence of the surface state, as proposed by Bardeen.⁽¹⁾

FIGURE CAPTIONS

Figure 5: The anomalous part of the frequency shift for an aluminum cavity and the effect of an applied magnetic field. Thermal expansion has been subtracted by fitting the data above 3.8 K. The field was applied in 12 Gauss steps perpendicularly to the endplate which produced the anomaly. Note that the curve at 180 Gauss lies very nearly on the thermal expansion extrapolation.

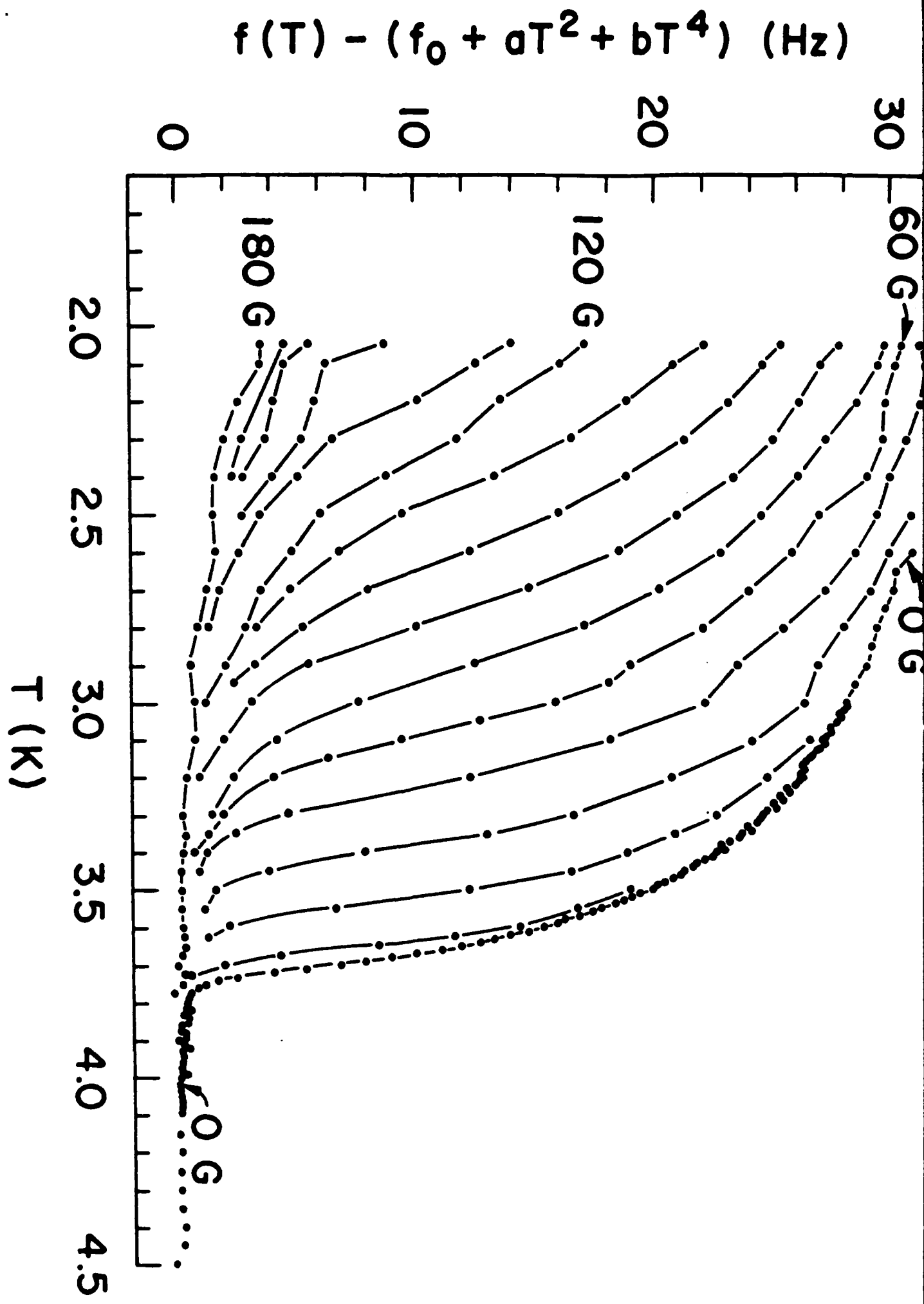
Figure 6: The anomalous part of the frequency shift for a copper cavity and the effect of an applied magnetic field. Thermal expansion has been subtracted by fitting the data above 7.1 K.

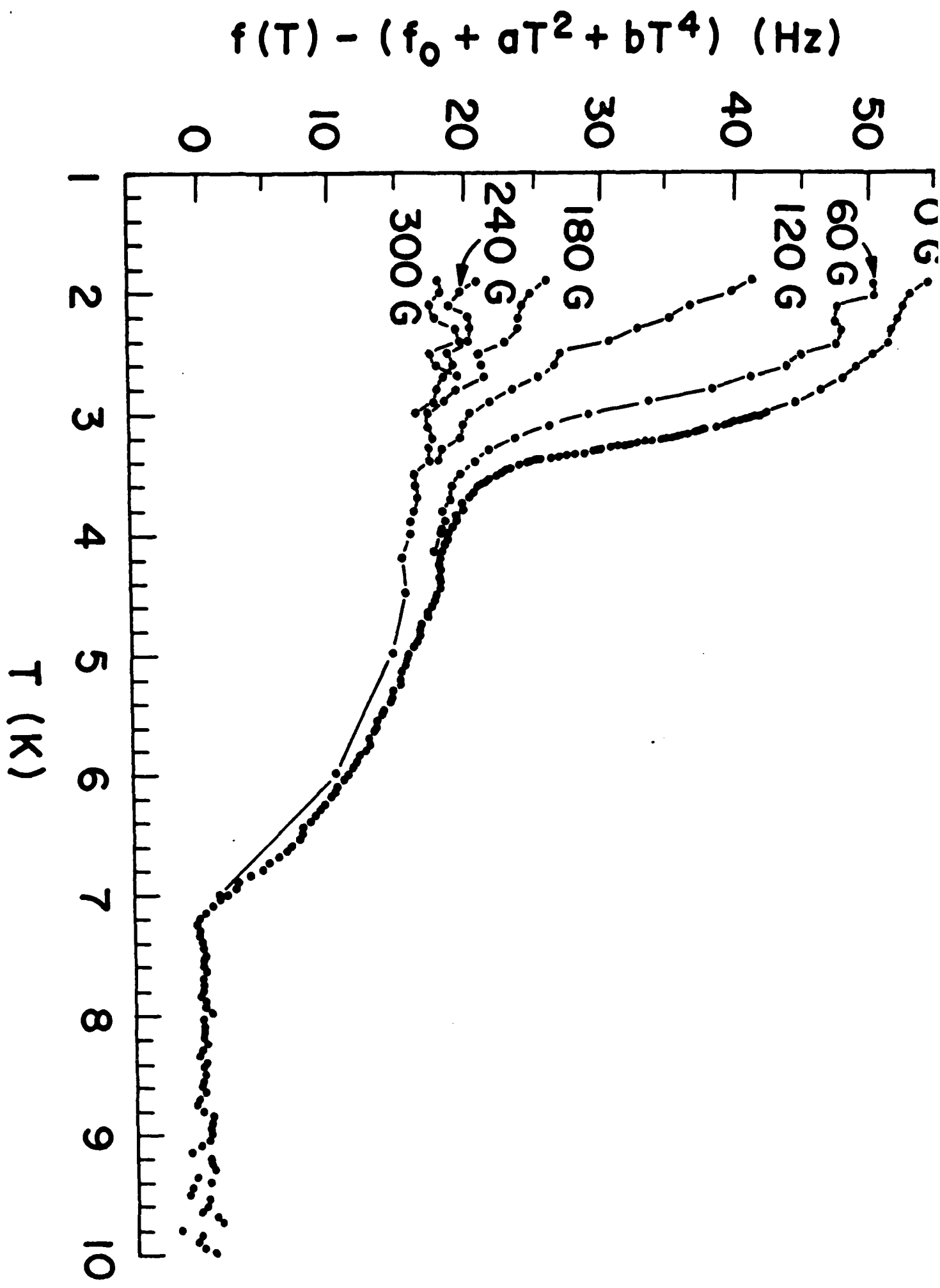
Figure 7: The derivative of the frequency shifts for a copper cavity, with thermal expansion subtracted. Above, cavity clean. Below, cavity with a thin layer of vacuum grease on its interior surface. The same thermal expansion fit was subtracted in each case.

Figure 8: The frequency shift and increased power absorption with an applied magnetic field near the cyclotron field. Note that the features on the two measurements align.

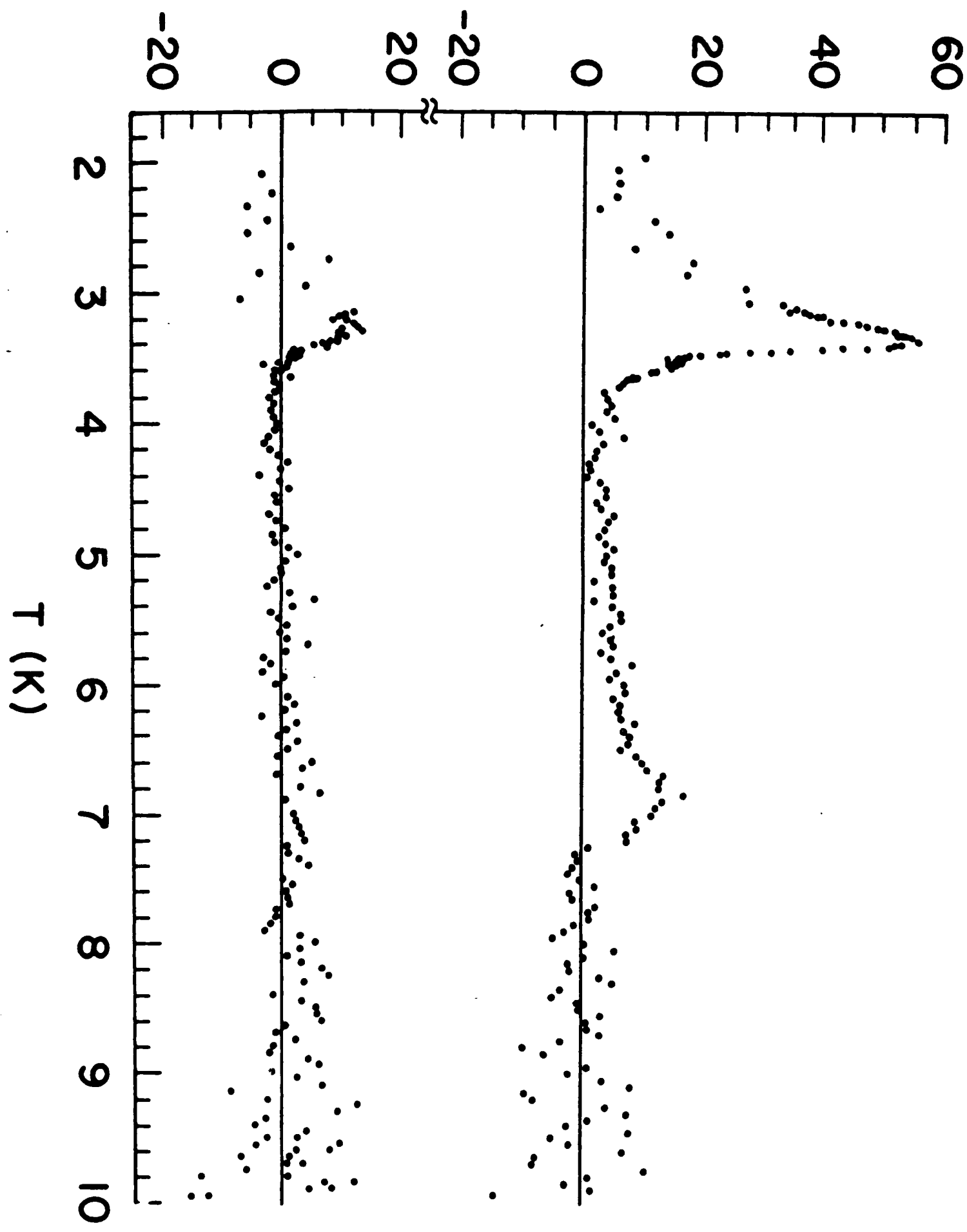
Figure 9: The height of the resonant peak as a function of incident microwave power. The two features of Figure 4 are plotted separately. Note the same slopes but different threshold powers. The threshold power level is of the order of one milliwatt.

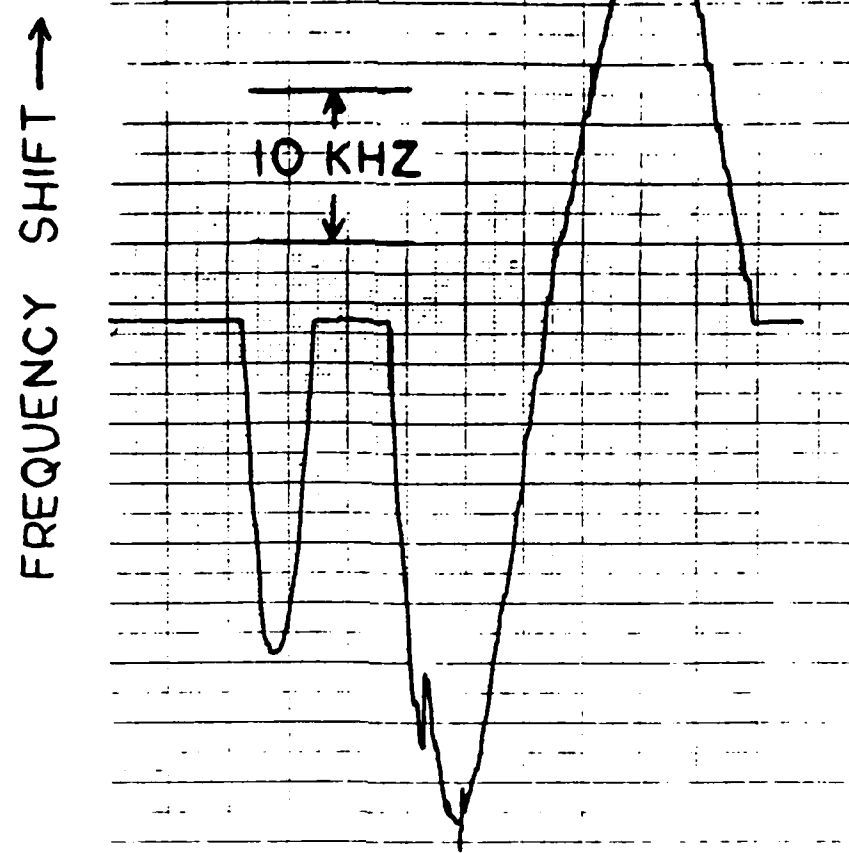
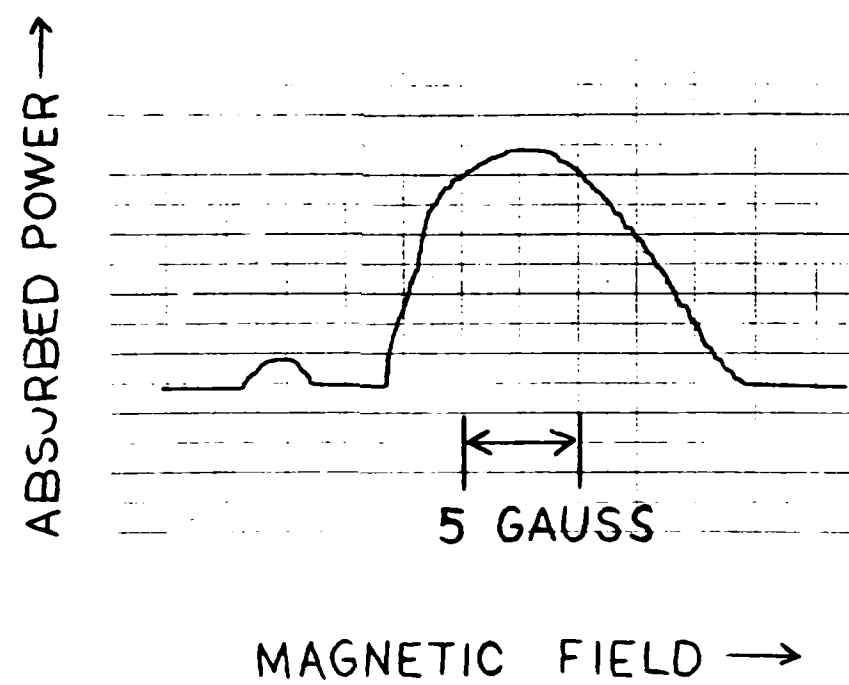
Figure 10: The smaller feature of Figure 8, near the power threshold. The magnetic field axis is greatly enlarged. Note the "switching" between the nonresonant state on the low field side of the resonance.

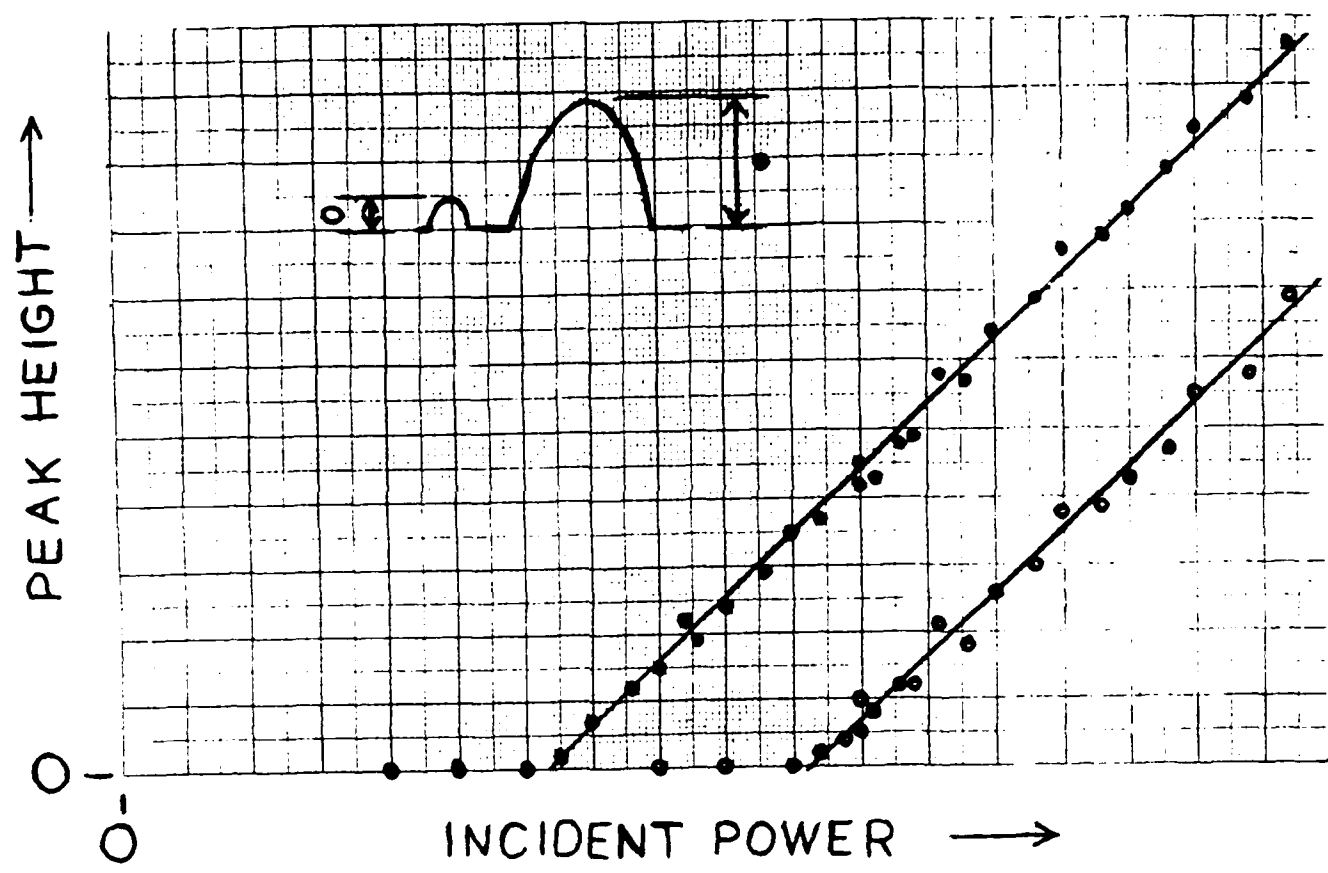




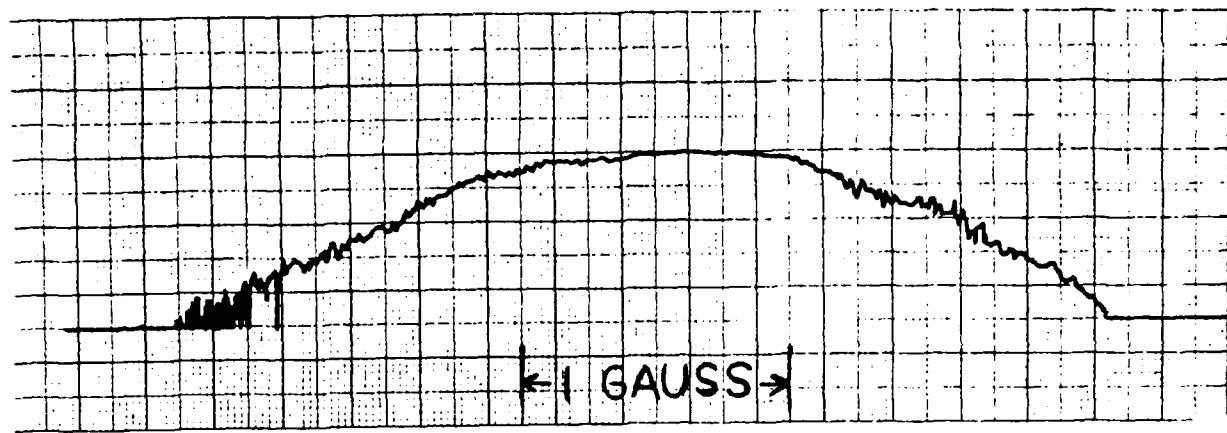
$$(\Delta f / \Delta T) = (2aT + 4bT^2) \text{ (Hz/K)}$$







ABSORBED POWER →



MAGNETIC FIELD →

THE ELECTRON FREE FALL EXPERIMENT

BACKGROUND

Motivated by the desire to measure for the first time the force of gravity on antimatter, Witteborn and Fairbank (WF)²⁷ developed a low temperature experiment to measure the force of gravity on individual electrons and positrons. The experiment has been successful on electrons. Due to advances in positron thermalization^{35,36,37} and the potential availability of an intense pulsed source of low energy positrons from the Stanford X-Ray Center Linac it now appears possible to complete in no more than three years the first measurement of the force on gravity on positrons.

The experiment uses a vertically oriented drift tube. In order to reduce stray electric fields, the copper tube was specially prepared to have small crystal size and a highly polished interior. WF found the net force exerted on electrons travelling along the axis of the tube to be zero to within $\pm 6 \times 10^{-12}$ V/m. (The force of gravity corresponds to a force of 5.6×10^{-11} V/m downward.) This was in conflict with theoretical expectations of a force of 10^{-6} to 10^{-5} V/m from patch effect fields and gravitational compression of the ionic lattice.

Using an apparatus (see Appendix 1) designed for variable temperature work, Lockhart, Witteborn and Fairbank (LWF)²⁸ found the room temperature value of the on-axis electric field in the copper tube to be $\sim 10^{-5}$ V/m. As the temperature of the tube is lowered to 4.5 K, the electric field drops to 3×10^{-7} V/m. Below this temperature the ambient field drops suddenly to 5×10^{-11} V/m. This is the value of the electric field expected from the compression of the electrons in the

tube by gravity. The electric field cancels the force of gravity on the electrons, so the net force is zero.

There are two main expected contributions to the ambient electric field in a vertical metal tube. The first is a spatially fluctuating field due to the contact potential differences between different crystallites on the surface of the tube. This "patch effect" field is expected to have an rms magnitude of about 10^{-6} V/m if the crystallites are randomly distributed. Secondly, gravitational distortion of the ionic lattice and the electron gas of the metal will produce a uniform axial electric field. Initially Schiff and Barnhill²⁹ calculated the magnitude of this gravitationally induced field to be mg/e , where m is the electron mass. Later, Dessler et. al.³⁰ showed the lattice compression should produce a field Mg/e where M is the ionic mass. The discrepancy between the two predictions was resolved by Herring³¹ when he showed the result of Dessler et al. could be obtained using the approach of Schiff and Barnhill by taking into account certain surface effects. The field expected to be seen was 10^{-6} - 10^{-7} V/m due to gravitational distortion of the ionic lattice.

From 300 K to 4.5 K the experimental results are consistent with the patch effect field and ionic lattice compression. The anomalous surface shielding seen at 4.5 K where the ambient electric field drops by almost four orders of magnitude is not yet understood. A central question in this work is to determine why the drift tubes show a transition in the shielding effect. Recent results with RF cavities (Appendix 4) indicate that the effect may take place on aluminum surfaces as well as on copper surfaces. We are trying to determine the

importance of such variables as oxide thickness, surface contaminants, and surface crystal size and orientation. We are using several approaches which allow us to look at a greater number of surfaces to test for enhanced surface shielding (Appendix 5).

Any attempt to explain the results of these experiments must be concerned primarily with accounting for why the patch effect and ionic lattice distortion fields are apparently shielded below 4.5 K, while the electron gas compression field apparently is not. Another consideration is that an electric field generated by running an axial current through the tube is seen by electrons travelling along the axis of the tube. Condensation of gas on the tube walls is not expected to be significant since less than 10^{-4} of a monolayer could condense during cooldown from the room temperature pressure of less than 10^{-9} torr. A study of the copper surface indicated that the copper oxide layer was approximately 20 Angstroms thick.

Hanni and Madey³² have evaluated the properties of surface electrons as a two-dimensional lattice, and as a thin Bose film. From room temperature to 5 K the experimental results are consistent with an ideal electron gas of density 10^{11} electrons/cm² on the surface of the copper oxide. The surface shielding transition at 4.5 K could be explained by the electrons forming Bose pairs with their image charges in the substrate and undergoing Bose condensation, although the predicted condensation temperature is considerably lower than 4.5 K.

A. R. Hutson³³ has proposed that electrons from the slow electron beam are captured on the surface of the oxide layer and are sufficiently mobile to shield the patch effect fields.

John Bardeen³⁴ has recently proposed that positively charged hole states on the surface of the copper oxide layer can undergo a transition to a metallic state at 4.5 K. These surface states are coupled to the interior of the copper by electron tunneling through the oxide. This maintains the Fermi level of the surface layer the same as that of the electrons in the copper.

RECENT WORK

In the WF experiment gravitational cutoffs were observed in ions (Figure 11) which gave a value of $g = 980 \pm 15\% \text{ cm/s}^2$. In the WF and LWF experiments with electrons the net force on the electrons was measured by analyzing the affect of known applied forces on the electron time of flight.

In order to more directly measure the energy of the electrons we have modified the experiment to use reflected electrons. After sending a pulse of electrons into the drift tube an electrode at the far end of the drift tube is made to reflect any electrons leaving the drift tube during a time interval from τ to $\tau + \Delta\tau$. These electrons are reflected again at the other end of the drift tube. They are then permitted to travel to the detector (in the original direction of travel). This results in a peak of electrons arriving at the detector during a time interval 3τ to $3(\tau + \Delta\tau)$. This technique allows us to separate truly slow electrons from electrons emitted from electro-magnetic traps at delayed times (WF and LWF showed that the electrons from traps do have low enough energies to be useful, but an uncertain time of emission from the trap). By varying the time of the reflection pulses and looking for the peak from reflected electrons we can directly measure the energy of those electrons, since we know their velocity. Figure 12 shows such a reflected peak. The first three points are the trailing end of the initial distribution. The region labelled "peak" around 0.4 msec is where the reflected peak is expected and seen. The electrons above the noise level following the peak are from traps populated by the reflected electrons. The data in Figure 12 is from a run at 77 K and corresponds

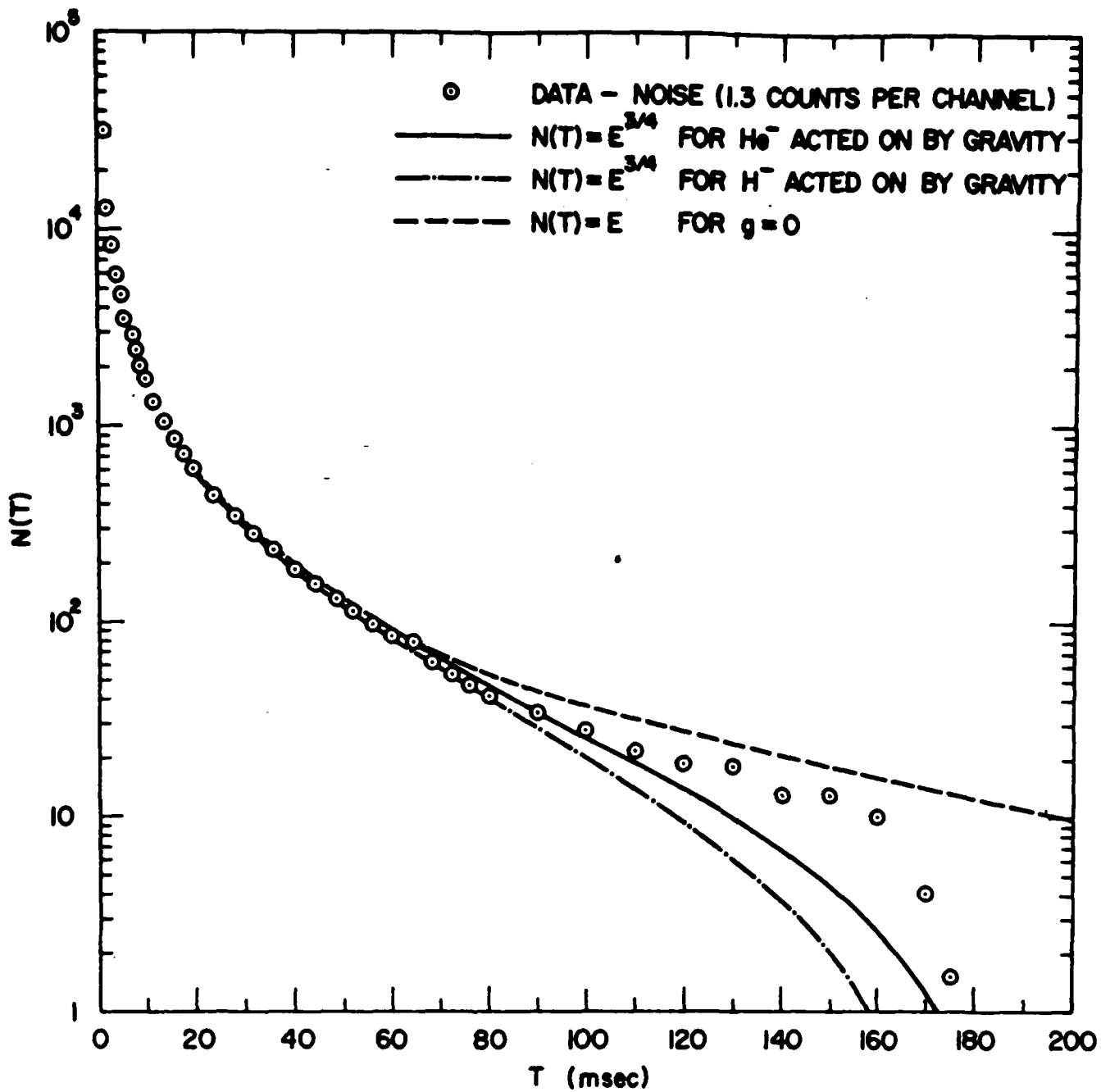
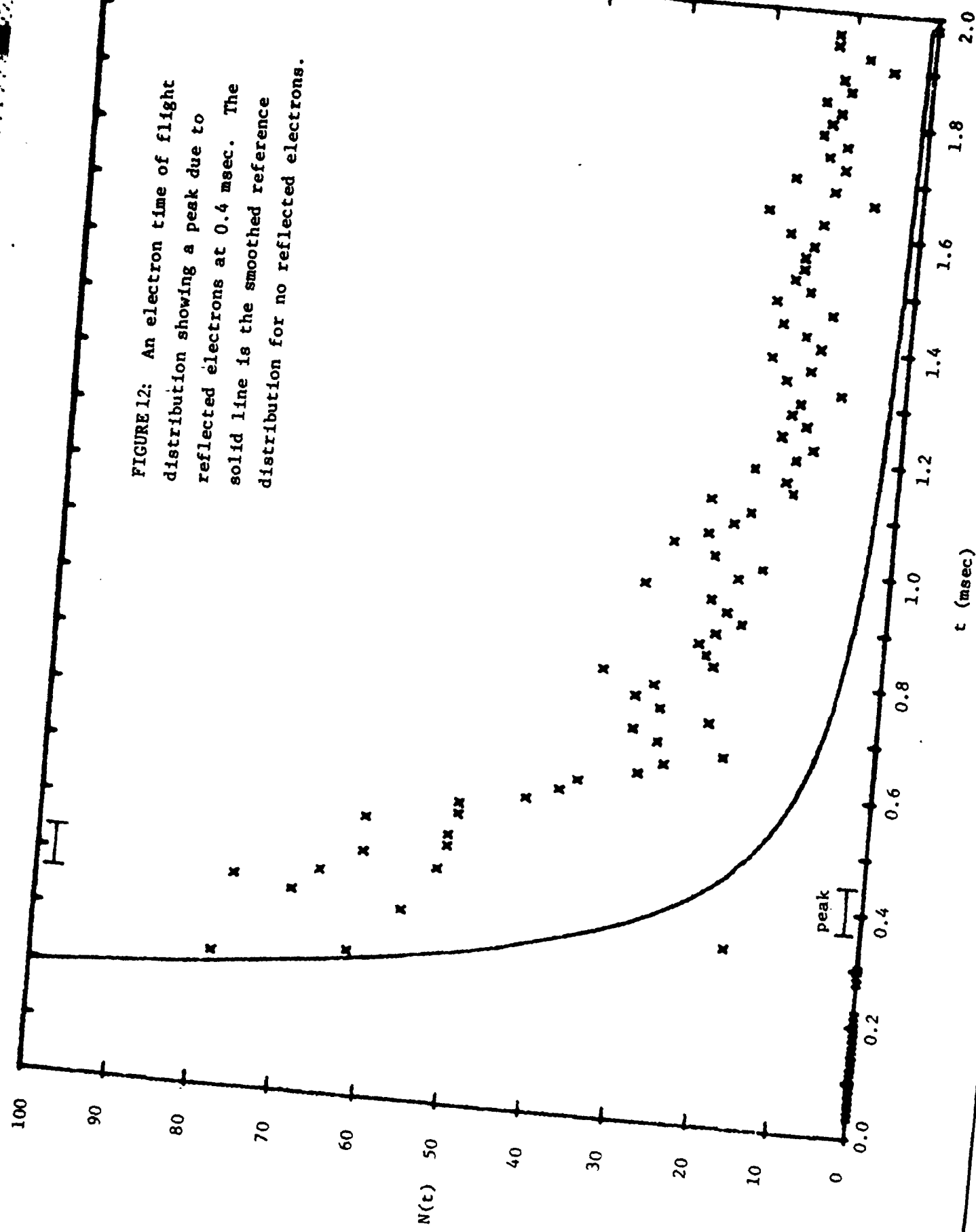


FIGURE 11. Time of flight data compared with expected distributions for a charged particle without a gravitational interaction, He^+ with an ordinary gravitational attraction, and H^- with ordinary gravitational attraction. (semilog plot) Magnetic forces are assumed negligible.

FIGURE 12: An electron time of flight distribution showing a peak due to reflected electrons at 0.4 msec. The solid line is the smoothed reference distribution for no reflected electrons.



to electrons with energies of 7×10^{-5} eV. Other preliminary data at 77 K show the presence of 1.7×10^{-5} eV electrons.

POSITRONS

The results of this experiment are relevant to theoretical arguments against the existence of "antigravity" - a repelling gravitational force between matter and antimatter. There are, however, no direct experimental tests of the gravitational forces on antimatter.³⁸ Having measured the force of gravity on electrons, a measurement using positrons would give the first measurement of the force of gravity on antimatter as well as giving a definitive value for the electrostatic shielding seen in the copper drift tube. In the electron experiment we measure no force on the electrons except that due to the applied electric field. We therefore conclude that the force of gravity on the electron is cancelled by an electric field due to the sag of the surface electrons in the gravitational field of the earth. If this is true, then the electric field will give a force on positrons in the direction of gravity and we will be able to verify both the gravitational force on positrons and electrons and the value of the ambient electric field in the tube. This would represent, in our opinion, a classic experiment that would remain a cornerstone in the history of gravity and absolute proof that the unusual shielding effect seen with the electrons has to exist.

To obtain slow positrons for this experiment we have been involved in a research program to develop a source of slow positrons. This work is discussed in the Ph.D. thesis of Glen Westenskow, included as Appendix 6. During the last few years there has been a rapid growth of

experiments which use low energy positrons to study a wide variety of problems in condensed matter physics. These experiments have become possible because of the development of procedures to moderate the energy of high energy positrons³⁵, including the pioneering work of John Madey on this project. However, most of these experiments, as well as our own, are limited by the small flux of low energy positrons. Since the flux of slow positrons is proportional to the initial flux of high energy positrons, source performance will be optimized when using an intense initial positron source. While our efforts have previously assumed the use of a natural β^+ emitter, there is now the possibility of using the MKIII linear accelerator at the Stanford X-Ray Center (SXRC).

We plan to use one of the positron beam ports that have been proposed for the SXRC. Positrons will be produced by pair production using the accelerator's first accelerating section. The first section is designed to produce a 45 MeV energy electron beam, to have a 10 μ sec long macropulse, and to yield 200 mA average current during the macropulse. A single pulse from the accelerator will consist of about 1.2×10^{13} electrons. The electron-positron conversion and the first thermalization stage will need to be done within the radiation shielding of the accelerator. Since the energy spread of the positron pulse from the converter is large and has a high angular dispersion, the efficiency of the first stage of thermalization will be low. Experiments to produce slow positrons with a 100 MeV accelerator at Livermore suggest that we may get better than 10^{-6} slow positrons per incident electron.³⁶ This will give about 10^7 positrons with about a 0.5 eV bandwidth. This

positron beam will then be accelerated to about 1 KeV for transport to the free-fall experiment.

A beam line will need to be constructed to transfer the near mono-energetic positrons to the free-fall apparatus. Since the beam will only be pulsed once per second the beam line need not be shielded, as the average radiation produced will be small even though the peak positron current is large. The 1 KeV positron beam can consist of simpler optics for transport than do most accelerator sections. To ensure a high vacuum in the free fall apparatus (10^{-10} Torr while operating at 4 K) several stages of differential pumping with several narrow apertures, consistent with the emittance of the beam, will be used.

Present plans are to inject the beam into the free fall apparatus from the top onto the axis of the drift tubes to a target located in the bottom section. This will require modifications to the existing vacuum pumping and particle detection systems. A detector will be modified to allow a narrow 1 KeV beam to pass through its center while still being sensitive to the wider return beam. The magnetic field along the free-fall axis will help guide the positron beam to the target. A higher strength magnetic field near the target, which is concentric with the free-fall drift tubes, will help to focus the beam into a tight spot to lower the emittance of the re-emerging positron beam.

The target will probably consist of a very clean single crystal copper sample. Under operation the block will be cooled to near 4 K. Other experiments have shown that this will yield a re-emitted positron beam with a very narrow energy bandwidth proportional to $(3/2)kT^{37}$. The

target vacuum will need to be isolated from the free-fall drift tubes under initial clean-up procedures. The surfaces which have given the best results in other experiments have usually been cleaned with Ar+ bombardment and then baked at 600-900 C for several hours. This will be done before the apparatus is inserted into the dewar. The 1 KeV positron will be thermalized to about 5×10^{-4} eV energy spread through interactions at a mean depth of a few hundred Angstroms. With a ~10% efficiency we would have 10^6 positrons in a 10 μ sec pulse (thermalization processes typically take place in less than 10^{-10} sec).

An increase in the number of very low energy particles can be achieved with some loss in timing. Since a low energy particle will take ~100 msec to travel the length of the free-fall drift tubes, the pulse can be stretched to 10 msec without degradation of the statistics. The particles that reemerge from the target can be trapped and stored in a magnetic-electrostatic trap. By slowly raising the bias of the center section of the trap with respect to the end gate, which is held at nearly the same potential as the free fall tubes, a very low energy beam ($\sim 10^{-8}$ eV) can be obtained which will have suitable characteristics for the experiment. The pulsed nature of the positron source allows opening the trap to admit a pulse of positrons and closing it again before they return to the entrance gate and escape. This should enhance the number of slow positrons with transverse energy below 10^{-10} eV to about 10^3 per pulse.

Since only slow positrons in the magnetic ground state can be used in the experiment there will be a 5 kG solenoid magnet around the target. This will separate the cyclotron states by 6×10^{-5} eV so that

the number of positrons in the magnetic ground state will be about 10^2 per pulse.

This procedure should be capable of yielding a higher number of positrons below 10^{-10} eV than is needed to perform the experiment. No more than one magnetic ground state positron with transverse energy below 10^{-9} eV is desired per pulse since the mutually repulsive forces between slow particles is larger than the gravitational force to be measured. With proper adjustment it should be possible to produce an average of about one such slow particle per pulse.

PROPOSED RESEARCH

ELECTRON FREE FALL

We propose to complete the set of experiments that are presently being performed. These experiments include measurements with ions instead of electrons. This will allow the separation of the contributions from gravitational and electrical fields by comparing results for beam particles with different charge-to-mass ratios. Prototype experiments with He^+ ions indicated an unexpectedly long lifetime of approximately 170 msec (Figure 11). Those measurements will be repeated with the present apparatus with better resolution. Another result from the earlier experiments that will be resolved is the dependence of the shielding effect on the axial magnetic field. Previously, it had been found that slow electrons were not present at high guiding fields, i.e., there was either no shielding effect or an electromagnetic trap was created that deflected the slow electrons from the beam. Using the guide solenoid over a range of magnetic fields and the reflected pulse technique, the magnetic dependence of the level of shielding will be systematically studied.

Simultaneous with the above experiments, we propose to complete construction of the beam line to carry low energy positrons from the MKIII accelerator to the free fall experiment; to build the low energy positron thermalizer; and to set up the required electrical connections, refrigerant transfer and recovery lines, and mechanical support structure for the experiment.

Upon completion of the present experiments we propose to move the apparatus to the MKIII accelerator, to modify the apparatus to make

measurements on positrons and to connect the apparatus to the low energy positron outlet of the MKIII accelerator. We plan to test the modified apparatus with electrons by Fall of 1986. After completing tests with positrons, we propose to alternate running the experiment with positrons and then with electrons. This would let us null out any nongravitational effects.

In light of the importance of a direct measurement of gravitational forces on antimatter and that the ambient forces in our experimental configuration are well characterized, the research proposed here would be free of the ambiguities which can arise from simultaneous gravitational, electric, and magnetic forces on a charged particle.

REFERENCES

1. John Bardeen, "Comments on Shielding by Surface States," in Near Zero: New Frontiers of Physics, to be published.
2. R. S. Hamm and J.M.J. Madey, Phys. Rev. 17B, 1976 (1978).
3. K. W. Rigby and W. M. Fairbank, Proc. 17th Int. Conf. on Low Temp. Phys. Part II, p. 1363, North-Holland (1984).
4. J. R. Henderson and W. M. Fairbank, Proc. 17th Int. Conf. on Low Temp. Phys. Part II, p. 1359, North-Holland (1984).
5. C. C. Grimes and G. Adams, Phys. Rev. Lett. 42, 795 (1979).
6. C. C. Grimes, T. R. Brown, Michael L. Burns and C. L. Zipfel, Phys. Rev. B 13, 140 (1976).
7. D. Straub and F. J. Himpsel, Phys. Rev. Lett. 52, 1922 (1984).
8. D. P. Woodruff, S. L. Hulbert, and P. D. Johnson, Phys. Rev. B 31, 4046 (1985).
9. G. A. Haas and R. E. Thomas, J. Appl. Phys. 48, 86 (1977).
10. Vacuum tunneling
11. R. Butz and H. Wagner, Appl. Phys. 13, 37 (1977).
12. L. B. Harris and J. Frasson, J. Phys. E, 17, 788 (1984).
13. M. Wolff, A. E. Guile and D. J. Bell, J. Phys. E, 2 (1969).
14. James H. Parker, Jr., and Roger W. Warren, Rev. Sci. Inst. 33, 948 (1962).
15. N. D. Lary and W. Kohn, Phys. Rev. B 3, 1215 (1971).
16. D. H. Darling and P. B. Pipes, Physica 85B, 277 (1977).
17. A. Th. A. M. deWaele, R. de Bruyn-Ouboter and P. B. Pipes, Physica 65, 587 (1973).

18. T. Ando et. al., Rev. Mod. Phys. 54, 437 (1982).
19. E. Etz et. al., Phys. Rev. Lett. 53, 2567 (1984).
20. Y. Goldstein et. al., Phys. Rev. B 19, 2256 (1979).
21. B. M. Vul and E. I. Zavaritskaya JETP 49, 551 (1979).
22. J. G. Gay et. al., Phys. Rev. Lett. 42, 332 (1979);
R. A. Bartynski et. al., Phys. Rev. B 31, 4745 (1985).
23. N. Garcia et. al., Phys. Rev. Lett. 54, 591 (1985).
24. C. C. Grimes and G. Adams, Phys. Rev. Lett. 42, 795 (1979).
25. M. W. Cole, Phys. Rev. B 2, 4239 (1970).
26. T. R. Brown and C. C. Grimes, Phys. Rev. Lett. 29, 1233 (1972).
27. F. C. Witteborn and W. M. Fairbank, Phys. Rev. Lett. 19 (1967)
1049.
28. J. M. Lockhart, F. C. Witteborn and W. M. Fairbank, Phys. Rev.
Lett. 38 (1977), 1220.
29. L. I. Schiff and M. V. Barnhill, Phys. Rev. 151 (1966), 1067.
30. A. J. Dessler, F. C. Michel, H. E. Rorschach, and G. T. Trammel,
Phys. Rev. 168 (1968), 737.
31. C. Herring, Phys. Rev. 171 (1968), 1361.
32. R. S. Hanni and J.M.J. Madey, Phys. Rev. B 17 (1978), 1976.
33. A. R. Hutson, Phys. Rev. B 1 (1978), 1934.
34. J. Bardeen, Comments on Shielding by Surface States, in Near
Zero: New Frontiers of Physics, to be published.
35. A. P. Mills, Jr., Appl. Phys. 22, 273-276 (1980).
36. P. J. Schultz and K. G. Lynn, Phys. Rev. B 26(5), (1982), 2390.
37. R. H. Howell, R. A. Alvarez and M. Stanek, Appl. Phys. Lett. 40(8)
(1982), 751.
38. T. Goldman and M. M. Nieto, Phys. Lett. 112B(6) (1982), 437.

END

FILMED

1-86

DTIC